



doi:10.1016/j.gca.2003.12.016

Speciation of strontium in particulates and sediments from the Mississippi River mixing zone

YINGFENG XU and FRANCO MARCANTONIO*

Department of Earth and Environmental Sciences, Tulane University, New Orleans, Louisiana 70118, USA

Abstract—Sequential extractions were performed on small amounts of particulate and sediment samples (6 to 10 mg) from the Mississippi River mixing zone. The leachates were analyzed for Sr concentration and $^{87}\text{Sr}/^{86}\text{Sr}$ isotope ratio. Mn and Fe contents were also measured as their oxyhydroxides are potential carrier phases for Sr. The largest fraction of Sr in the solid phase (particulates and sediments) was found to be present in the residual, refractory fraction (>70% of total). By comparison with the corresponding sediment, particulates appear to have higher concentrations of nonresidual, labile Sr (30% vs. 15%). Carbonate components seem to play an important role as carriers for labile Sr in particulates and sediments. Changes in the composition and content of the solid phase may significantly modify both the $^{87}\text{Sr}/^{86}\text{Sr}$ isotope ratio of the total labile fractions and that of the bulk components. However, such modifications, under normal conditions, exert little measurable influence on the Sr isotope composition of the dissolved phase. Copyright © 2004 Elsevier Ltd

1. INTRODUCTION

The $^{87}\text{Sr}/^{86}\text{Sr}$ isotope ratio of marine sediments has long been used as a proxy in stratigraphic correlation and global climate change studies (e.g., Broecker and Peng, 1982; Burke and Denison, 1982; McKenzie et al., 1988; Raymo, 1991; Ingram and Sloan, 1992; Andersson et al., 1994; Patterson et al., 1995; Derry and France-Lanord, 1996; Huh and Edmond, 1998; Denison et al., 1998; Harris et al., 1998; Vaiani, 2000). The crucial assumption that lies behind these applications is that Sr is chemically and isotopically uniform in seawater because of its long residence time (2–5 Ma) compared to the mixing time of water in the oceans ($\sim 10^3$ yr) (Brass, 1976; Burke and Denison, 1982; McArthur, 1991; Henderson et al., 1994; Capo et al., 1998). However, more recent studies have suggested that small but considerable regional differences in both flux and isotopic composition of Sr can occur on time-scales shorter than its residence time (Andersson et al., 1994; Derry and France-Lanord, 1996; Stoll and Schrag, 1998; de Villiers, 1999). Nonconservative behavior of Sr has been observed in estuaries (Andersson et al., 1994; Wang et al., 2001), in which various dynamic processes may control and modify the transport of fluvial material to the oceans. The degree to which Sr behaves nonconservatively in estuaries needs to be better understood to interpret more fully oceanic Sr isotopic archives.

Given that Sr is mainly present in the dissolved pool of aquatic systems, and that Sr isotopes are not fractionated by any natural chemical or biologic process, the conventional view is that the $^{87}\text{Sr}/^{86}\text{Sr}$ ratio in the estuarine water column only changes by conservative mixing of distinct water masses during transport to the oceans. However, an investigation of fresh and brackish waters in the Baltic Sea (Andersson et al., 1994) has shown that Sr can be redistributed by Fe-Mn oxyhydroxides in the water column, i.e., formation of Fe-Mn oxyhydroxide par-

ticulates scavenges Sr from the dissolved load, while dissolution of Fe-Mn particulates under suboxic-anoxic conditions releases Sr back to the dissolved load. They also found that removal of Sr by Fe-Mn oxyhydroxides tends to decrease the usually large differences in $^{87}\text{Sr}/^{86}\text{Sr}$ ratio between particulate and dissolved loads. Another study on Changjiang (Yangtze River) estuarine waters (Wang et al., 2001) has shown that strong water-sediment interaction might account for observed increases in the $^{87}\text{Sr}/^{86}\text{Sr}$ ratio of the dissolved phase.

Here we perform sequential extraction analyses on particulate (>0.2 μm) and surface sediment samples from the Mississippi River (MR) mixing zone in an attempt to investigate the inventory of Sr in solid phases and its potential influence on the behavior of Sr in the estuarine environment. Sequential extraction is a chemical technique in which a series of digestions are performed on one solid sample in an effort to extract different components of elements of interest (e.g., the Sr adsorbed onto the Fe-Mn-oxyhydroxide component; the Sr bound to organic matter, etc.). Although the value of this technique has been debated over the past two decades because of concerns over readsorption and incomplete selectivity (e.g., Nirel and Morel, 1990), useful insights have been gained on the partitioning, association, and source-history of trace elements (Chester and Hughes, 1967; Kersten and Forstner, 1986; Tessier and Campbell, 1991; Koschinsky and Halbach, 1995; Ouddane et al., 1997; Perin et al., 1997; Dong et al., 2000). Most studies using sequential leaching techniques have been performed on either large sediment samples (1 g or more) (Kersten and Forstner, 1986; Perin et al., 1997; Alvarez et al., 2001), or on particulates that were filtered from large volumes of water (Ouddane et al., 1997; Roux et al., 1998). This study, for the first time, to our knowledge, sequentially extracts trace elements from milligram-sized samples of particulates and sediments. Although the sequential extraction of trace elements from sediments is not usually limited by the availability of sample material, the same cannot be said for particulate samples. In general, particulate samples obtained through filtration on site during field work are small, especially for saline water (often less than 20 mg/47-mm

* Author to whom correspondence should be addressed (fmarcan@tulane.edu).

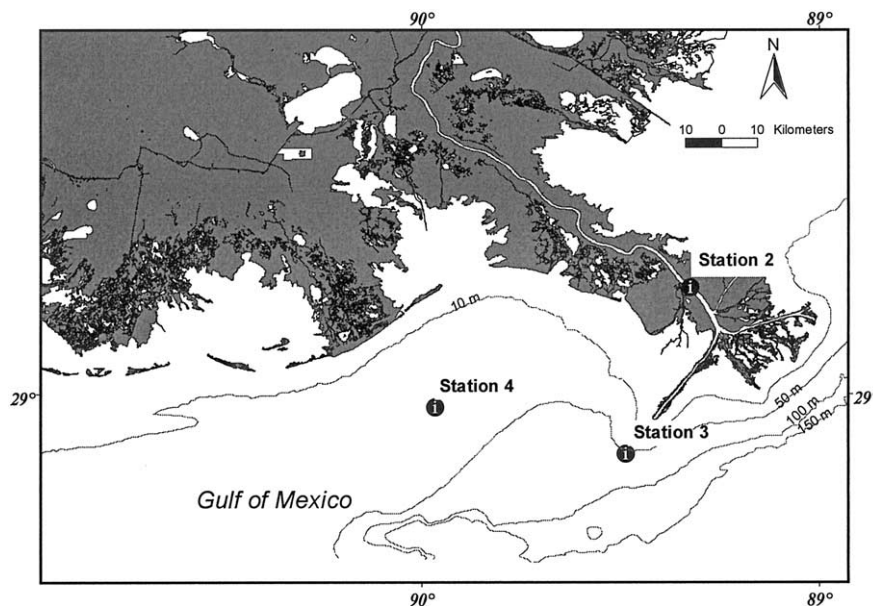


Figure 1. Location map of the samples. Surface and bottom particulates, and surface sediment were retrieved from Station 2 in the river channel. Surface sediment was retrieved from Stations 3 (at the mouth of river at SW pass) and 4 (in the outflow region).

filter). Our motivation, therefore, for testing the sequential extraction method on small samples is to find a practical way to look further into the distribution of elements in particulates, which we believe can provide more information about an element's geochemistry than traditional bulk digestions. To our knowledge, it is also the first investigation of Sr speciation within the various components of particulates and sediments in an estuarine environment. Such information is important to the construction of a Sr oceanic budget and any assessment of the Sr isotope records archived in marine sediments.

2. SAMPLING AND ANALYTICAL METHODS

Surface and bottom waters and sediments were sampled within the mixing zone of the MR in July 1999 (Fig. 1). Surface particulate, bottom particulate, and surface sediment samples were retrieved from the MR channel (Station 2). Two additional surface sediment samples were collected at the MR mouth (Station 3) and to the west of the mouth within the west bight (Station 4). The surface particulate sample was collected from water with a salinity of 0.04‰ and suspended particulate matter (SPM) concentration of 120 mg/L. The bottom particulate sample was collected from water with a salinity of 0.2‰ and SPM concentration of 363 mg/L. The salinity of the overlying waters at Station 3 and Station 4 was 36.3‰ and 35.9‰, respectively. Water samples were filtered on the research vessel through 0.2 μm Millipore Isopore polycarbonate membrane filters. The particulate filters (trapping $>0.2 \mu\text{m}$ suspended particles) were stored in acid-cleaned holders. Sediment samples were collected with a box corer and sectioned immediately within a nitrogen-pressurized glove box. After being transported back to the lab, the particulate samples were dried at 40°C inside an oven. The sediment samples were freeze-dried and ground homogeneously.

The sequential extraction procedure is based on the methods of Tessier (Tessier et al., 1979) and Roux (Roux et al., 1998) and modified for small samples (6–10 mg). Successive sequential leachings of each sample were processed in the same acid-cleaned 2-mL centrifuge tube, except for the last extraction, in which the sample was transferred to a Teflon vial for strong-acid and high-temperature processing. Each particulate or sediment sample has had the following four fractions

extracted from it. The volume of reagents used in each step is for a 10-mg sample. The actual volume of reagents was scaled according to the weight of each sample.

1. The ion-exchangeable and carbonate fractions (F1): One ml of 1M CH_3COONa , adjusted to a pH of 5.0 with CH_3COOH , was added to the sample and shaken at room temperature for 1 h. The leachate was separated by centrifugation at 4000 RPM for 10 min. The supernatant (for F1) was extracted by pipette. The residue was washed with 0.5 mL of de-ionized (DI) water to reduce the effect of residual reagent on the next step.
2. The reducible fraction (F2) containing the Mn-oxides and amorphous Fe-oxides: Two ml of 0.02M $\text{NH}_2\text{OH} \cdot \text{HCl}$ in 25% (v/v) CH_3COOH was added to the residuals from the first step and shaken at room temperature for 4 h. After centrifugation and extraction (as in 1) of the supernatant (F2) by pipette, the residue was washed with 0.5 mL of DI water.
3. The organic fraction (F3) containing the organic matter, and perhaps, some sulfides: One ml of 30% H_2O_2 adjusted to a pH of 2.0 with HNO_3 was added to the residuals from the second step and shaken occasionally at room temperature for 4 h. Centrifugations and extraction of F3 was performed as in steps 1 and 2.
4. The residual fraction (F4) containing the lithogenic crystalline minerals, and perhaps, a small amount of refractory organic matter: Two ml of concentrated HF and 1 mL of HNO_3 was added to the residual solid and heated at $\sim 100^\circ\text{C}$ overnight.

To minimize contamination, sample preparations and sequential extractions were performed under class 100 clean conditions. Elemental concentrations were measured on the Element 2 inductively coupled plasma mass spectrometer at Tulane. For Sr isotope analysis, samples were purified by ion exchange chromatography using Sr-specific resin from Eichrom™ at Tulane and measured by thermal ionization mass spectrometry at Florida State University. The average $^{87}\text{Sr}/^{86}\text{Sr}$ ratio of five measurements of the Eimer and Amend (E & A) Sr standard during the course of our study (Table 1) was 0.708006 ± 0.000009 (2σ).

Blank corrections, measured for each element in each sequential extraction step, were no greater than 3% in all cases except for a few leachates of F1, that were $\sim 7\%$. The reproducibility of our sequential extraction method was examined with duplicate analyses. The small differences in element concentrations between the replicates (Table 2)

Table 1. Sr isotope standard (E&A) measurement.

E&A	$^{87}\text{Sr}/^{86}\text{Sr}$	2SE ^a
std 1-1	0.708002	0.000009
std 1-2	0.708007	0.000010
std 2-1	0.708004	0.000008
std 2-2	0.708013	0.000010
std 3-1	0.708006	0.000010
Mean	0.708006	0.000009

^a Standard error of the mean.

demonstrates: (a) the stability and precision of this method; and (b) the homogeneity of the small samples processed.

3. RESULTS

3.1. Elemental Results

The concentrations of Sr, Mn, and Fe from each leachate are listed in Table 3. Note that for the surface particulate sample, the sums of the concentrations of the sequential extracts do not match well with measured bulk concentrations for each trace element. This was most likely the result of an analytical artifact during transfer of the residual fraction (F4) to a different container for digestion purposes (see Section 2). Since the residual fraction is expected to be a nonreactive component, we believe that the low accuracy of the trace element concentrations in F4 for the surface particulate sample is insignificant to our interpretation below.

For all the samples, the residual fraction (i.e., F4) contains the majority of the Sr (70–87%) and Fe (84–92%). In contrast the nonresidual, and potentially most labile, fraction (i.e., F1, F2, and F3) contains the majority of the Mn (59–77%).

For Sr, the particulate samples, 2S and 2B, have higher concentrations of the nonresidual fractions than the sediment samples, 2SED, 3SED and 4SED (Fig. 2). Nonresidual Sr is largely associated with F1, which may account for up to 80% of the total nonresiduals with a mean of $\sim 72 \pm 7\%$. About 13 to 24% of the total nonresidual Sr is associated with F2, which is expected to represent the Mn-Fe oxide fraction. Additionally, ~ 4 to 10% is in F3, the organic-bound fraction.

Mn concentrations in the nonresidual fractions are dramatically higher in the particulates than in the sediments, especially for the reducible fraction, F2 (Fig. 3). In addition, Mn concentrations in F3 are higher for the particulate samples than for the sediment samples. For the sediment samples, Mn is distributed in similar proportions between F1 and F2 (both $\sim 40\%$ of the nonresidual fractions), while the organic-bound Mn fraction (F3) plays a less important role ($<20\%$).

Despite the low percentage of total nonresidual Fe (8 to 16%), its absolute amount is much higher than nonresidual Mn (compare Figs. 3 and 4). For the total nonresidual components, the concentration of Fe is ~ 4 times and 6 to 23 times that of Mn for particulates and sediments, respectively. For the organic fraction alone this ratio is even higher, i.e., ~ 12 to 60. Nonresidual Fe is mainly present in F2 and F3 (~ 40 – 58% for both). Fe in F1 is very low, representing only 1 to 4% of the total nonresidual fractions.

3.2. Sr Isotopic Results

$^{87}\text{Sr}/^{86}\text{Sr}$ isotope ratios for both particulate and sediment samples increase with further successive leaching. The $^{87}\text{Sr}/^{86}\text{Sr}$ ratios in F3 are distinctly higher than those in F1 and F2. For all the samples, each labile fraction has lower $^{87}\text{Sr}/^{86}\text{Sr}$ ratios than that of its bulk sample (Table 3).

Particulate and sediment nonresidual $^{87}\text{Sr}/^{86}\text{Sr}$ isotopic ratios are plotted against inverse Sr concentrations in Figure 5. The data display a broad negative relationship between the isotopic ratio and concentration of Sr (within two lines in Fig. 5). Data for the residual fractions are also added to this plot for comparison. These fractions lie far off of the array defined by the nonresiduals and are characterized by extremely high Sr concentrations and $^{87}\text{Sr}/^{86}\text{Sr}$ ratios (Fig. 5).

4. DISCUSSION

4.1. Sr Partitioning and Relationships with Mn and Fe

Nonresidual Sr has been found to occur largely in F1. The F1 fraction represents the total of the ion-exchangeable and carbonate fractions of the particulate and sediment matter. To differentiate between these two potential constituents of F1, we performed an “ion-exchangeable test” on one of our particulate samples by leaching with DI water. Our test showed that $\sim 16\%$ of Sr in F1 ($\sim 3.6\%$ of the total particulate Sr) can be released by DI water. Since seawater, the actual reactant in nature, has an extremely high ionic strength, an even higher proportion of exchangeable Sr is expected. Although our DI water leaching experiment cannot distinguish between the relative importance of the two components that make up F1, it does provide for a minimum baseline for the ion-exchangeable fraction. If one assumes that the ion-exchangeable Sr makes up 50% of F1, the ion-exchangeable and carbonate components would each make up $\sim 37\%$ of the total nonresidual Sr in the particles. If the carbonate component of F1 is mainly biogenic, the amount of Sr bound in this fraction may be higher in the summer high-productivity season than during other seasons.

Sr associated with Mn-Fe oxides comprises $\sim 18\%$ of the total nonresidual fractions on average, that is similar to or significantly lower than the Sr associated with the ion-exchangeable and/or carbonate fraction. A study by Andersson et al. (1994) has shown that Fe-Mn oxyhydroxides can trap Sr as they form. This sequential extraction experiment shows that carbonates play a comparable, or more important, role as a carrier phase for Sr in particles. The component that has the

Table 2. Element concentrations ($\mu\text{g}/\text{g}^{\text{a}}$) in duplicate analyses.

Sample	Wt mg	Fraction	Sr	Mn	Fe
2B	8.75	F1	26.7 ± 0.4	134 ± 1	37.0 ± 0.3
		F2	5.7 ± 0.2	471 ± 9	1298 ± 5
		F3	1.99 ± 0.02	119 ± 1	$1427 \pm .2$
		F4	81.2 ± 0.8	212 ± 2	$32.2 \pm 0.3^{\text{a}}$
2B	8.69	F1	25.1 ± 0.4	119 ± 5	31 ± 1
		F2	6.1 ± 0.1	422 ± 4	1268 ± 37
		F3	2.38 ± 0.01	131.4 ± 0.2	1529 ± 8
		F4	81 ± 1	226 ± 3	$34.9 \pm 0.4^{\text{a}}$

^a Fe concentration in residual fraction is given in mg/g.

Table 3. Sr, Mn, and Fe distribution in each sequential extraction (concentration units: $\mu\text{g/g}$ for particulate and sediment samples^a; $\mu\text{g/l}$ for dissolved water samples).

Station	Location	Sample	Fraction	$^{87}\text{Sr}/^{86}\text{Sr}$	2SE ^b	Sr	Mn	Fe	
2	89.291W 29.260N	SP	F1	0.709458	± 0.000012	30 ± 2	162 ± 3	51.8 ± 0.8	
			F2	0.709480	± 0.000025	4.9 ± 0.2	366 ± 8	1272 ± 9	
			F3	0.711164	± 0.000039	1.67 ± 0.01	74.1 ± 0.5	1104 ± 6	
			F4	0.723779	± 0.000055	60 ± 1	185 ± 4	28.5 ± 0.2^a	
		SD	Bulk		0.718485	± 0.000015	137.4 ± 0.4	1401 ± 16	45.6 ± 0.2^a
					0.709570	± 0.000017	187 ± 2	1.00 ± 0.03	12.7 ± 0.2
					0.709432	± 0.000010	26.7 ± 0.4	134 ± 1	37.0 ± 0.3
					0.709493	± 0.000021	5.7 ± 0.2	471 ± 9	1298 ± 5
		BP	F1		0.710768	± 0.000035	1.99 ± 0.02	119 ± 1	1427 ± 12
					0.723703	± 0.000024	81.2 ± 0.8	212 ± 2	32.2 ± 0.3^a
					n/a		132 ± 1	1299 ± 23	36.7 ± 0.4^a
					0.709596	± 0.000009	194 ± 1	0.43 ± 0.02	2.7 ± 0.1
		Sediment	F1		0.709615	± 0.000058	13.0 ± 0.4	125 ± 5	71.8 ± 0.7
					0.709813	± 0.000022	4.7 ± 0.1	140 ± 3	1030 ± 2
				0.710729	± 0.000080	1.390 ± 0.001	43.1 ± 0.1	808 ± 4	
				0.719519	± 0.000046	123 ± 2	133 ± 3	16.8 ± 0.1^a	
3	89.486W 28.840N	Sediment	F1		0.717444	± 0.000009	140 ± 1	767 ± 6	23.0 ± 0.1^a
					0.709596	± 0.000009	19.0 ± 0.3	98 ± 4	194 ± 1
					0.710031	± 0.000021	4.3 ± 0.1	83.2 ± 0.7	3011 ± 21
					0.712247	± 0.000024	2.0 ± 0.1	37.5 ± 0.9	1959 ± 3
		Bulk	F2		*0.722840		81.2 ± 0.4	142 ± 1	26.6 ± 0.4^a
					0.719757	± 0.000037	100.8 ± 0.5	533 ± 7	36.9 ± 0.4^a
					0.709109	± 0.000010	18.0 ± 0.4	80 ± 2	41.6 ± 0.1
					0.709742	± 0.000017	5.7 ± 0.2	75 ± 2	1453 ± 5
		Sediment	F3		0.711235	± 0.000152	2.87 ± 0.01	35 ± 1	2085 ± 5
					*0.717805		121 ± 1	131 ± 1	23.3 ± 0.2^a
					0.716307	± 0.000008	146.5 ± 0.2	524 ± 6	32.6 ± 0.5^a

^a Fe concentrations in residual fraction and bulk samples are given in mg/g.

^b Standard error of the mean.

SP = surface particulate; SD = surface dissolved; BP = bottom particulate; BD = bottom dissolved.

* Value derived by mass balance calculation.

least amount of the nonresidual Sr associated with it is F3, the organic matter fraction. It accounts for $\sim 7\%$ (4 to 10%) of the total nonresiduals.

The differences in the partitioning of Sr, Mn, and Fe among the nonresidual components reflect the differences in their biogeochemical behavior. Comparing the three samples from the river channel (i.e., 2S, 2B, and 2SED), the concentrations of Sr, Mn, and Fe all show a decrease in the nonresidual fractions from particulates to the sediment (Figs. 2, 3, and 4). This is not unexpected, as physical (e.g., compaction) and chemical (e.g.,

mineralization and remineralization) processes within the sediment tend to reduce the labile components in the solid phase. The differences are that both Mn and Fe have maximum nonresidual concentrations in the bottom particulate samples, while Sr has its maximum nonresidual concentration in the surface particulate sample. The higher concentrations of Mn in F2 and F3 lead to the maximum nonresidual Mn concentrations in the bottom particulate sample. The maximum nonresidual Fe concentration seems to result from the higher content of Fe in F3. For Sr, the dominant role of F1 determines the variability of

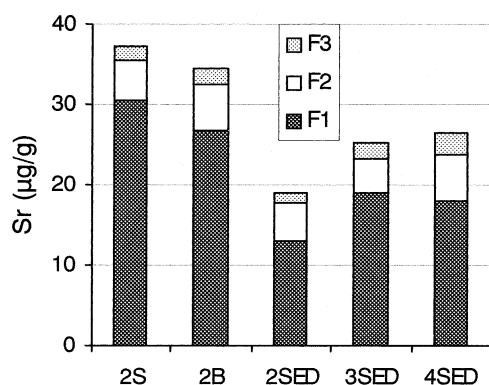


Figure 2. Nonresidual (labile) Sr concentrations (F1 = Ion-exchangeable and carbonate fractions; F2 = Reducible fraction; F3 = Organic fraction).

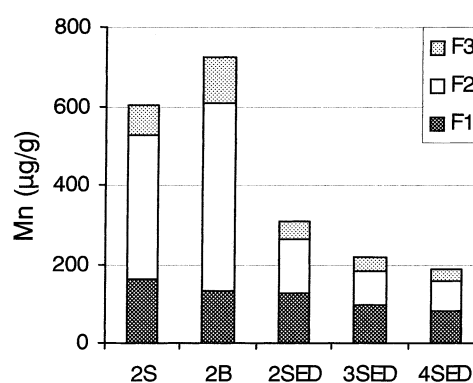


Figure 3. Nonresidual (labile) Mn concentrations (F1 = Ion-exchangeable and carbonate fractions; F2 = Reducible fraction; F3 = Organic fraction).

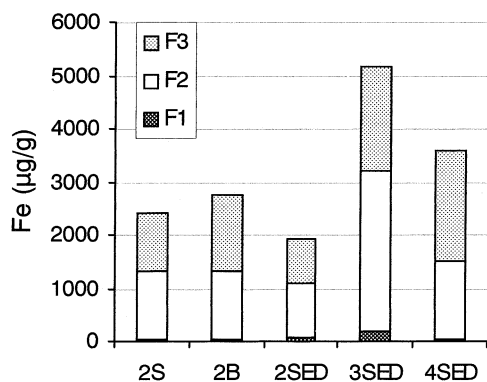


Figure 4. Nonresidual (labile) Fe concentrations (F1 = Ion-exchangeable and carbonate fractions; F2 = Reducible fraction; F3 = Organic fraction).

the total nonresidual concentrations between samples. The higher concentrations of Mn and Fe in the bottom particulates may be caused by precipitation of hydrous Mn-Fe oxides and organic particles, while the higher Sr concentration in the surface particulates may be the result of higher phytoplankton production in the surface-water column.

Comparing the three sediment samples, the concentrations of Sr, Mn, and Fe in the nonresidual components vary differently. Sr concentrations are higher in the sediment samples from the outflow region (i.e., 3SED and 4SED) than in the sample from the river channel (i.e., 2SED, Fig. 2). The total nonresidual Fe (mostly in F2 and F3) concentrations are also higher in the

sediment samples from the outflow region (Fig. 4). In contrast, Mn concentrations are highest in the river channel sediment (Fig. 3). The higher concentrations of nonresidual Sr and Fe in the outflow region may be due to the relatively higher proportions of finer-grained sediment that usually have greater concentrations of nonresidual components. The lower Mn concentrations in the outflow region may result from suboxic chemical conditions that cause some Mn to be released from the sediments while not affecting Fe, which needs stronger reducing conditions to be remobilized. This seems to be supported by the lower concentrations of Mn (Fig. 3) and higher Fe concentrations in F2 for the outflow region samples (Fig. 4). In addition to the variations in F2, a decrease of Mn in F1 (Fig. 3) and an increase of Fe in F3 in the outflow region (Fig. 4) also contribute to the spatial variations of the total nonresidual Mn and Fe concentrations.

The higher nonresidual Sr concentrations in the outflow region sediment samples are mainly derived from F1 (Fig. 2). This augmented Sr in F1 might be largely ascribed to a high-carbonate component. Although this source of labile Sr seems to predominate in our study, a role for Mn-Fe oxyhydroxides in the cycling of Sr cannot be precluded, given their dynamic chemical properties.

4.2. Controls on the Sr Isotopic Composition of Labile Components

Although $^{87}\text{Sr}/^{86}\text{Sr}$ isotope ratios for both particulate and sediment samples increase with further successive leaching

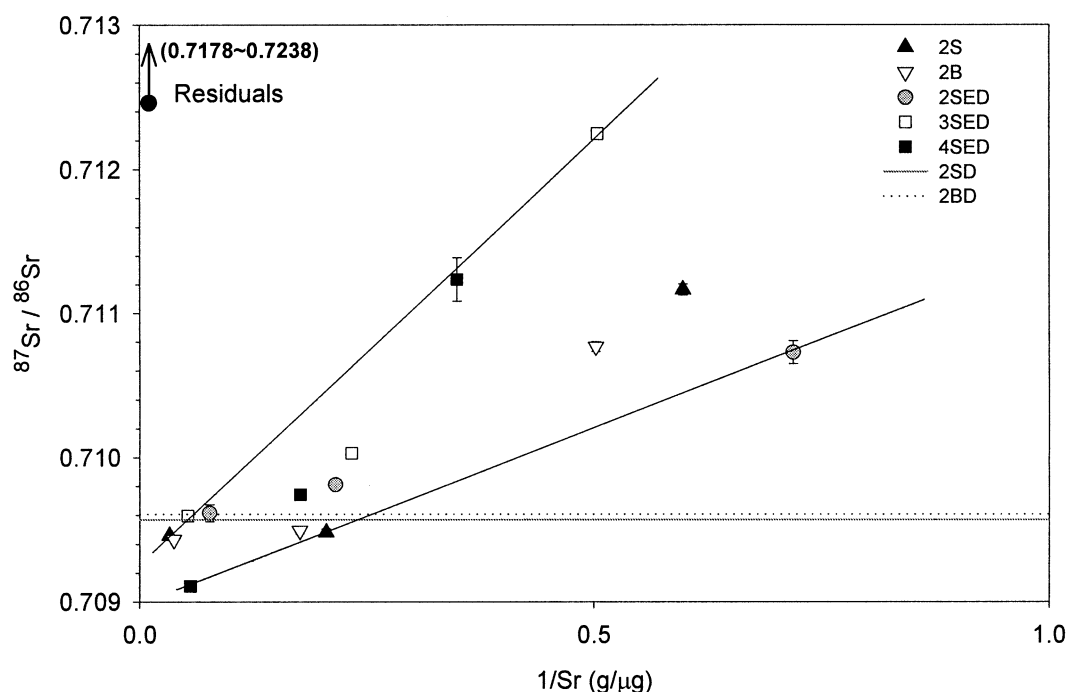


Figure 5. Sr isotopic systematics of the leachates. All the points representative of the nonresidual fractions fall within the outlined mixing array. Horizontal lines represent the Sr isotopic compositions of dissolved phases of Station 2; 2SD = surface dissolved; 2BD = bottom dissolved. The black dot with an arrow in the upper left corner indicates the general position of the residual fractions in this diagram. 2S = surface particulate of Station 2; 2B = bottom particulate of Station 2; 2SED = surface sediment of Station 2; 3SED = surface sediment of Station 3; 4SED = surface sediment of Station 4.

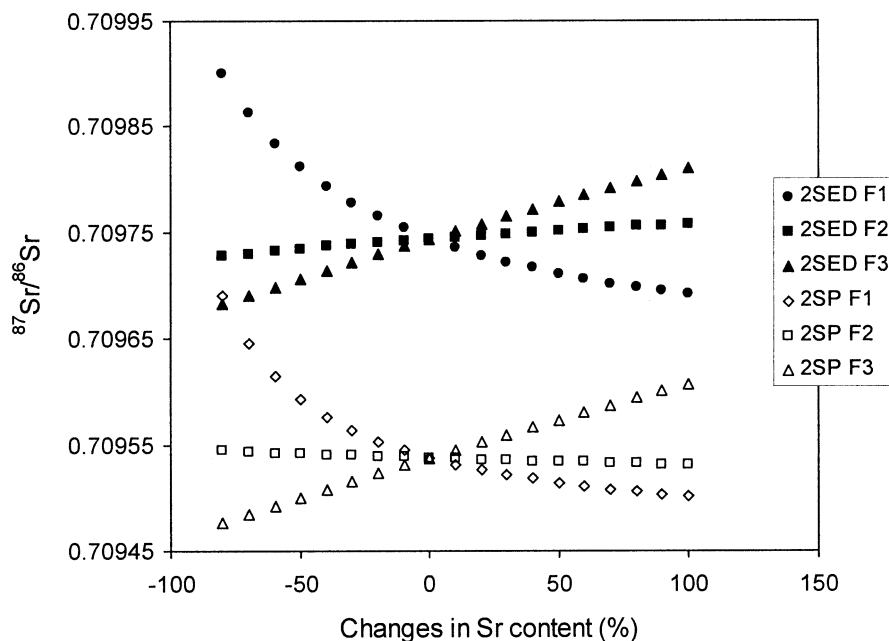


Figure 6. Modeled control of Sr concentration changes on Sr isotopic composition of the total nonresidual fractions. The nonfilled symbols represent the surface particulate sample of Station 2. The bottom particulate sample at Station 2 has a similar pattern and is not shown. The filled symbols represent the Station 2 surface sediment sample and are also indicative of the patterns for the surface sediment samples of Station 3 and Station 4. Positive numbers on the X-axis indicate gain of a nonresidual fraction to the solid phase, while negative numbers indicate loss.

(Table 3 and Fig. 5), variations in $^{87}\text{Sr}/^{86}\text{Sr}$ ratios for each nonresidual leachate in different samples do not covary with those of the residual leaches. Moreover, the Sr isotopic compositions of the residual fractions are far off of the binary mixing array defined by the nonresidual fractions. This evidence indicates that factors other than attack of the residual fraction (most radiogenic) account for these changes.

For the two particulate samples, the $^{87}\text{Sr}/^{86}\text{Sr}$ ratios of F1 and F2 are slightly lower than the dissolved load isotope ratio (Table 3). The slightly lower $^{87}\text{Sr}/^{86}\text{Sr}$ ratios in these fractions may be due to a variety of factors: (1) the scavenging particles draw Sr from a “truly dissolved” pool that has a lower $^{87}\text{Sr}/^{86}\text{Sr}$ ratio than the arbitrarily defined dissolved load ($<0.2\ \mu\text{m}$); (2) the slightly higher dissolved phase $^{87}\text{Sr}/^{86}\text{Sr}$ ratio is caused by the release of more radiogenic Sr from particulates; (3) the carbonates in F1 represent detrital/ancient marine carbonates that have lower $^{87}\text{Sr}/^{86}\text{Sr}$ ratio; and (4) phosphates from fertilizers contribute to the lower $^{87}\text{Sr}/^{86}\text{Sr}$ of F1 (Martin and McCulloch, 1999). We believe that (3) and (4) can be ruled out; when one compares the $^{87}\text{Sr}/^{86}\text{Sr}$ ratios of the particulates and the sediment at Station 2 (Table 3), the Sr isotope signature of F1 for the sediment sample does not agree with the Sr isotope signature for the particulate samples. If the less radiogenic sources for Sr are derived from ancient marine detritus and/or fertilizer-associated phosphates, the surface sediments most likely should have preserved the less radiogenic signature of Sr. There is support for the first scenario in research performed by Douglas et al. (1995), in which the $^{87}\text{Sr}/^{86}\text{Sr}$ ratios in the different size fractions of particulates from five rivers of the Murray-Darling River system of Australia were measured. They found that the Sr isotopic ratio decreases as the particle

size decreases in size fractions that range from greater than $1\ \mu\text{m}$ to less than $0.003\ \mu\text{m}$. Colloids remaining in the arbitrarily defined dissolved load may preserve the more radiogenic Sr isotope signature from further upstream. If this is the case, then one might infer that colloids are important in the regulation of the isotope signature of fluvial Sr that makes its way into the oceans. Although we have no evidence for any mechanism which might allow scenario (2), we cannot rule it out.

Given that each labile fraction has lower $^{87}\text{Sr}/^{86}\text{Sr}$ ratios than that of the bulk sample, addition of the labile components always decreases, while loss of these components increases, the $^{87}\text{Sr}/^{86}\text{Sr}$ ratio of the bulk sample. When one considers only the labile fractions (i.e., nonresidual), the effects that loss or gain of any labile fraction have on the total labile Sr isotopic ratio can be seen in our modeling analysis in Figure 6. Each evolution curve for the $^{87}\text{Sr}/^{86}\text{Sr}$ ratio of the total labile fractions is formed by changing the Sr content of one of the three labile fractions (in percentage of the concentration measured here), while keeping the other two unchanged. For example, curve 2SP-F1 illustrates the variability of $^{87}\text{Sr}/^{86}\text{Sr}$ ratio of the total labile components in the surface particulates upon increasing or decreasing the Sr content of F1 (as a percentage of the total $30\ \mu\text{g/g}$ concentration measured) without changing the amount of F2 and F3. For both the particulate and sediment samples, addition of F1 always decreases, while addition of F3 always increases, the $^{87}\text{Sr}/^{86}\text{Sr}$ ratio of the total labile components. Differences are encountered when gain/loss models of F2 of the particulate samples are compared to those in the sediment samples. Specifically, addition of F2 to the particulates slightly decreases the $^{87}\text{Sr}/^{86}\text{Sr}$ ratio of the total labile components (Fig.

6a), while addition of the same fraction to the sediments slightly increases the Sr isotope value (Fig. 6b).

Figure 6 also schematically illustrates the differences between the Sr isotopic compositions of the total labile components of the particulates versus those of the sediments. Compared to the particulates, the sediments have more radiogenic Sr isotope signatures (~ 200 ppm), an indication that the sediments have undergone some degree of diagenetic processing.

The broad relationship between Sr concentration and Sr isotope ratio in Figure 5 suggests that the Sr isotope signatures of the labile components are determined from two general sources. One has a high Sr concentration and a low Sr isotope ratio (the lowest $^{87}\text{Sr}/^{86}\text{Sr}$ ratios in the water column). We hypothesize that source likely represents the truly dissolved pool from which the exchangeable ions adsorb and the carbonate particles form. The isotopic composition of this truly dissolved pool might be expected to vary in response to spatial or salinity variations. The other source has a low Sr concentration and a high Sr isotope ratio, and is most likely an organic constituent. The observed $^{87}\text{Sr}/^{86}\text{Sr}$ ratios of F3 are higher than those measured in lower-MR water (0.71009; Xu, unpublished data). Since natural processes do not fractionate Sr isotopes, the high $^{87}\text{Sr}/^{86}\text{Sr}$ ratios of F3 in the estuarine mixing zone may be explained by the preservation of more radiogenic signatures from further upstream in the mixing zone. We speculate that the second source relates to terrigenous detrital organic matter derived from land soils. It is also possible that a slight leaching of the siliceous residual fraction (at pH = 2) contributes to the high $^{87}\text{Sr}/^{86}\text{Sr}$ ratios of F3.

4.3. Implications for Sr Flux and Isotopic Systematics

The MR drains 45% of the conterminous United States delivering 6.2×10^{11} kg/yr of suspended solids to the delta and Gulf of Mexico (Coleman et al., 1998). Based on this study, $\sim 30\%$ Sr in the particulates is labile, more than 75% of which is present in F1. Meanwhile, $\sim 16\%$ of F1 can be desorbed by DI water. This means that 3.6% or so of the Sr contained in the total suspended particulate matter is releasable by DI water. Despite the high ion-strength of seawater that may favor the desorption process, we conservatively assume that 5% of SPM Sr is ion-exchangeable with seawater. Hence desorption of Sr from SPM can account for an additional 3.1×10^9 g/yr of Sr delivered to the Gulf of Mexico during mixing of river water with seawater. This number equals $\sim 4.6\%$ of the MR fluvial Sr flux delivered in the dissolved load to the Gulf of Mexico, which is 6.8×10^{10} g/yr based on an annual average discharge of $450 \text{ km}^3/\text{yr}$ at the Tarbert Landing gauge (average of U.S. Geological Survey website data for 1935–2002), and an average river water Sr concentration of $\sim 150 \mu\text{g}/\text{L}$ (Xu, unpublished data).

The annual flux of Sr to the oceans via world rivers is $\sim 33.3 \times 10^9$ mol/yr with an average $^{87}\text{Sr}/^{86}\text{Sr}$ ratio of 0.7119 (Palmer and Edmond, 1989; Krishnaswami et al., 1992). Extrapolating our findings from the MR to global rivers, SPM may deliver an additional 1.5×10^9 mol/yr (1.3×10^{11} g/yr) of fluvial Sr to the oceans (or coastal regions). From our speciation results, we estimate that the $^{87}\text{Sr}/^{86}\text{Sr}$ ratio of this additional source to be slightly lower than that estimated for world rivers (~ 0.7115). This additional flux is larger than that of the dissolved Sr flux

from the MR and slightly less than one half of the benthic Sr flux from deep-sea sediments (3.4×10^9 mol/yr with a $^{87}\text{Sr}/^{86}\text{Sr}$ ratio of 0.7084; Palmer and Edmond, 1989). Due to the large inventory of Sr in the ocean, an additional SPM desorption source of Sr plays a minor role in the Sr isotope budget of the oceans.

Fine-grained particles deposited in coastal regions may represent another source of desorbed labile Sr to the oceans, especially when climatic variations in sea level occur. Based on data from this study, the Sr isotope ratio of shelf sediments can be similar to or less radiogenic than that of average rivers, but higher than that of ocean water. Sr concentrations in continental shelf sediments from this study are ~ 100 to $140 \mu\text{g}/\text{g}$. We estimate that the labile fractions of Sr exceed 10% of the total Sr in shelf sediments, of which the ion-exchangeable, carbonate and reducible components account for $\sim 90\%$, and the organic component accounts for $\sim 10\%$. During the last deglaciation approximately $28.9 \times 10^6 \text{ km}^2$ of the global continental shelf sediment was inundated with seawater because of melting ice sheets. Labile Sr stored in the sediment, at least that associated with ion-exchangeable and reducible components, is expected to be remobilized when exposed to elevated ion-strength seawater and, potentially, an increased extent of seasonal hypoxic/anoxic conditions. To see the effect of this labile Sr on the ocean Sr budget we can perform a simple calculation in which we assume that: (a) the inundation of $28.9 \times 10^6 \text{ km}^2$ of shelf area occurred within 10 ka; (b) a 50-cm thick of shelf sediment was involved in the Sr remobilization processes (due to erosion as a consequence of rapid sea level rise and penetration of seawater); and (c) 8% of the total Sr in the sediment was released. In this way, we estimate an export of 1.7×10^{12} mol of Sr during this 10 ka, averaging 1.7×10^8 mol annually, which is almost one order of magnitude smaller than the riverine particulate desorption flux. Therefore, a Sr flux from sediments seems to make an insignificant contribution to the oceanic Sr budget during deglacials. That the labile fractions of shelf sediments presumably would tend to have more radiogenic Sr isotope ratios than those of riverine particulates (200 ppm higher than the $^{87}\text{Sr}/^{86}\text{Sr}$ ratios of the corresponding particulates in this study, Table 3) complicates this conclusion.

Our study indicates that changes in the partitioning of Sr between dissolved and particulate (or sediment) phases do not seem to exert a direct, measurable influence on the Sr isotopic systematics of the dissolved phase. However, one could envision that strong seasonal changes in the geochemical environment (temperature, pH, Eh, salinity) of coastal sediment reservoirs, and episodic biologic and physical disturbances within such reservoirs (e.g., bioturbation, high-production-related anoxia, large storms, submarine slumps and slides), have the potential to release Sr from the labile components identified here. For example, potential influence on the dissolved load may take place as a result of postdepositional remobilization (e.g., resuspension), as observed in the Changjiang estuary (Wang et al., 2001). In addition, one might expect an influence when dissolution of particles occurs in regions that have distinctly low dissolved-load Sr isotope composition. In either case, the Sr flux from the labile components of the particulates has to be large enough to affect the dissolved phase.

Using our limited observations from a single world river, we can only speculate with respect to global oceanic Sr fluxes and

isotopic systematics. However, we consider this speculation to be a valid first-order attempt at trying to constrain the oceanic Sr cycle, given its importance to global change studies.

5. CONCLUSION

This study provides a first-order look of the inventory of Sr in the solid phases of an important estuarine mixing zone. The extent to which these solid phases influence Sr behavior during variable geochemical processing has been investigated. Our sequential extraction study indicates that, in addition to Fe-Mn oxyhydroxides (Andersson et al., 1994) carbonates seem to be another important carrier phase for mobile Sr in particulates and sediments. Changes in the contents of carbonates and organic matter may affect both the isotopic composition and elemental concentration of Sr in the solid phase. Changes in the concentration of the Fe-Mn component exert an insignificant effect on the Sr isotopic composition of the solids.

Changes in the partitioning of Sr between dissolved and particulate phases may not directly influence the Sr isotopic systematics of the dissolved phase. Potential influence on the dissolved load, however, may take place as a result of post-depositional remobilization, or when dissolution of the particles occurs in regions that have distinctly low dissolved-load Sr isotope compositions.

Our estimates of the labile Sr flux and isotopic systematics of the MR and global rivers, and our estimate of the labile Sr flux from sediments due to eustatic sea level rise, are rough and based on limited samples from a single sampling of the MR. We present these estimations in an attempt to shed light on the role which particulates and their labile fractions in estuarine environments play in regulating the oceanic Sr cycle. Better estimates would require similar research on riverine and estuarine systems from throughout the world.

Acknowledgments—We thank Tom Bianchi for inviting us to join the July 1999 Mississippi River cruise and Martha Sutula for providing us with the sediment samples. We thank Michael Bizimis, Afi Sachi-Kocher, Vincent Salters, and Leroy Odum for help in measuring Sr isotope ratios at FSU. S. Krishnaswami and H. Stoll provided useful and constructive reviews, as did two anonymous reviewers. This research is partly funded by Sigma Xi Grants-in-Aid of Research program from Sigma Xi, The Scientific Research Society and by a grant from the Tulane-Xavier Center for Bioenvironmental Research.

Associate editor: S. Krishnaswami

REFERENCES

- Alvarez M. B., Malla M. E., and Batistoni D. A. (2001) Comparative assessment of two sequential chemical extraction schemes for the fractionation of cadmium, chromium, lead and zinc in surface coastal sediments. *Fresenius J. Anal. Chem.* **369**, 81–90.
- Andersson P. S., Wasseberg G. J., Ingri J., and Stordal M. C. (1994) Strontium, dissolved particulate loads in fresh and brackish waters: the Baltic Sea and Mississippi Delta. *Earth and Planetary Science Letters* **124**, 195–210.
- Brass G. W. (1976) The variation of the marine $^{87}\text{Sr}/^{86}\text{Sr}$ ratio during Phanerozoic time: interpretation using a flux model. *Geochim. Cosmochim. Acta* **40**, 721–730.
- Broecker W. S. and Peng T.-H. (1982) *Tracers In The Sea*. Lamont-Doherty Geological Observatory of Columbia University.
- Burke W. H. and Denison R. E. (1982) Variation of seawater $^{87}\text{Sr}/^{86}\text{Sr}$ throughout Phanerozoic time. *Geology* **10**, 516–519.
- Capo R. C., Stewart B. W., and Chadwick O. A. (1998) Strontium isotopes as tracers of ecosystem processes: theory and methods. *Geoderma* **82**, 197–225.
- Chester R. and Hughes M. J. (1967) A chemical technique for the separation of ferro-manganese minerals carbonate minerals and adsorbed trace elements from pelagic sediments. *Chem. Geol.* **2**, 249–262.
- Coleman J. M., Roberts H. H., and Stone G. W. (1998) Mississippi River Delta: an overview. *Journal of Coastal Research* **14**, 698–716.
- Denison R. E., Koepnick R. B., Burke W. H., and Hetherington E. A. (1998) Construction of the Cambrian and Ordovician seawater $^{87}\text{Sr}/^{86}\text{Sr}$ curve. *Chem. Geol.* **152**, 325–340.
- Derry L. A. and France-Lanord C. (1996) Neogene Himalayan weathering history and river $^{87}\text{Sr}/^{86}\text{Sr}$: impact on the marine Sr record. *Earth and Planetary Science Letters* **142**, 59–74.
- de Villiers S. (1999) Seawater strontium and Sr/Ca variability in the Atlantic and Pacific oceans. *Earth and Planetary Science Letters* **171**, 623–634.
- Dong D., Nelson Y. M., Lion L. W., Shuler M. L., and Ghiorse W. C. (2000) Adsorption of Pb and Cd onto metal oxides and organic material in natural surface coatings as determined by selective extractions: New evidence for the importance of Mn and Fe oxides. *Wat. Res.* **34**, 427–436.
- Douglas G. B., Gray C. M., Hart B. T., and Beckett R. (1995) A strontium isotopic investigation of the origin of suspended particulate matter (SPM) in the Murray-Darling River system, Australia. *Geochim. Cosmochim. Acta* **59**, 3799–3815.
- Harris N., Bickle M., Chapman H., Fairchild I., and Bunbury J. (1998) The significance of Himalayan rivers for silicate weathering rates: evidence from the Bhote Kosi tributary. *Chem. Geol.* **144**, 205–220.
- Henderson G. M., Martel D. J., O’Nions R. K., and Shackleton N. J. (1994) Evolution of seawater $^{87}\text{Sr}/^{86}\text{Sr}$ over the last 400 ka: the absence of glacial/interglacial cycles. *Earth and Planetary Science Letters* **128**, 643–651.
- Huh Y. and Edmond J. M. (1998) On the interpretation of the oceanic variations in $^{87}\text{Sr}/^{86}\text{Sr}$ as recorded in marine limestones. *Proc. Indian Acad. Sci. (Earth Planet. Sci.)* **107**, 293–305.
- Ingram B. L. and Sloan D. (1992) Strontium isotopic composition of estuarine sediments as paleosalinity-paleoclimate indicator. *Science* **255**, 68–72.
- Kersten M. and Forstner U. (1986) Chemical fractionation of heavy metals in anoxic estuarine and coastal sediments. *Wat. Sci. Tech.* **18**, 121–130.
- Koschinsky A. and Halbach P. (1995) Sequential leaching of marine ferromanganese precipitates: Genetic implications. *Geochim. Cosmochim. Acta* **59**, 5113–5132.
- Krishnaswami S., Trivedi J. R., Sarin M. M., Ramesh R., and Sharma K. K. (1992) Strontium isotopes and rubidium in the Ganga-Brahmaputra river system: weathering in the Himalaya, fluxes to the Bay of Bengal and contributions to the evolution of oceanic $^{87}\text{Sr}/^{86}\text{Sr}$. *Earth and Planetary Science Letters* **109**, 243–253.
- Martin C. E. and McCulloch M. T. (1999) Nd-Sr isotopic and trace element geochemistry of river sediments and soils in a fertilized catchment, new South Wales, Australia. *Geochim. Cosmochim. Acta* **63**, 287–305.
- McArthur J. M. (1991) Stratigraphy with strontium isotopes. *Geology Today* **7**, 5i–5iv.
- McKenzie J. A., Hodell D. A., Mueller P. A., and Muller D. W. (1988) Application of strontium isotopes to late Miocene-early Pliocene stratigraphy. *Geology* **16**, 1022–1025.
- Nirel P. M. V. and Morel F. M. M. (1990) Pitfalls of sequential extractions. *Wat. Res.* **24**, 1055–1056.
- Ouddane B., Martin E., Boughriet A., Fischer J. C., and Wartel M. (1997) Speciation of dissolved and particulate manganese in the Seine river estuary. *Marine Chemistry* **58**, 189–201.
- Palmer M. R. and Edmond J. M. (1989) The strontium isotope budget of the modern ocean. *Earth and Planetary Science Letters* **92**, 11–26.
- Patterson R. T., Blenkinsop J., and Cavazza W. (1995) Planktic foraminiferal biostratigraphy and $^{87}\text{Sr}/^{86}\text{Sr}$ isotopic stratigraphy of the Oligocene-to-Pleistocene sedimentary sequence in the Southeastern Calabrian microplate, Southern Italy. *Journal of Paleontology* **69**, 7–20.

- Perin G., Fabris R., Manente S., Rebello Wagener A., Hamacher C., Scotto S. (1997) A five-year study on the heavy-metal pollution of Guanabara Bay sediments (Rio de Janeiro, Brazil) and evaluation of the metal bioavailability by means of geochemical speciation. *Wat. Res.* **31**, 3017–3028.
- Raymo M. E. (1991) Geochemical evidence supporting T.C. Chamberlin's theory of glaciation. *Geology* **19**, 344–347.
- Roux L. L., Roux S., and Appriou P. (1998) Behaviour and speciation of metallic species Cu, Cd, Mn and Fe during estuarine mixing. *Marine Pollution Bulletin* **36**, 56–64.
- Stoll H. M. and Schrag D. P. (1998) Effects of Quaternary sea level cycles on strontium in seawater. *Geochim. Cosmochim. Acta* **62**, 1107–1118.
- Tessier A., Campbell P. G. C., and Bisson M. (1979) Sequential extraction procedure for the speciation of particulate trace metals. *Analytical Chemistry* **51**, 844–851.
- Tessier A. and Campbell P. G. C. (1991) Comment on "Pitfalls of sequential extractions" by P. M.V. Nirel and F. M. M. Morel. *Wat. Res.* **25**, 115–117.
- Vaiani S. C. (2000) Testing the applicability of strontium isotope stratigraphy in marine to deltaic Pleistocene deposits: an example from the Lamone River Valley (Northern Italy). *Journal of Geology* **108**, 585.
- Wang Z., Liu C., Han G., and Xu Z. (2001) Strontium isotopic geochemistry of the Changjiang estuarine waters: Implications for water-sediment interaction. *Science In China (Series E)* **44**, 129–133.